

ESTIMATION OF ROTARY STABILITY DERIVATIVES AT SUBSONIC
AND TRANSONIC SPEEDS

By Murray Tobak and Henry C. Lessing

Ames Research Center
Moffett Field, Calif., U.S.A.

Presented to the Fluid Dynamics and Flight Mechanics
Panels of Advisory Group for Aeronautical
Research and Development

Brussels, Belgium
April 10-14, 1961

NASA FILE COPY
PLEASE RETURN TO CODE ETL
OFFICE OF TECHNICAL INFORMATION
AND EDUCATIONAL PROGRAMS
NATIONAL AERONAUTICS
AND SPACE ADMINISTRATION
Washington 25, D. C.

NATIONAL AERONAUTICS and SPACE ADMINISTRATION
WASHINGTON

SUMMARY

The first part of this paper pertains to the estimation of subsonic rotary stability derivatives of wings. The unsteady potential flow problem is solved by a superposition of steady flow solutions. Numerical results for the damping coefficients of triangular wings are presented as functions of aspect ratio and Mach number, and are compared with experimental results over the Mach number range 0 to 1.

In the second part, experimental results are used to point out a close correlation between the nonlinear variations with angle of attack of the static pitching-moment curve slope and the damping-in-pitch coefficient. The underlying basis for the correlation is found as a result of an analysis in which the indicial function concept and the principle of superposition are adapted to apply to the nonlinear problem. The form of the result suggests a method of estimating nonlinear damping coefficients from results of static wind-tunnel measurements.

CONTENTS

	Page
SUMMARY	i
FIGURE TITLES	iii
SYMBOLS	iv
1. INTRODUCTION	1
2. ESTIMATION OF $C_{L\dot{\alpha}}$ AND $C_{m\dot{\alpha}}$ FOR WINGS AT SUBSONIC SPEEDS	2
2.1 Solution to Potential Equation	3
2.2 Loading Coefficient	3
2.3 Solution for Triangular Wing	4
2.4 Approximate Steady-State Loadings	5
2.5 Empirical Corrections	8
3. DAMPING IN PITCH IN THE PRESENCE OF NONLINEAR STEADY-STATE FORCES AND MOMENTS	9
3.1 The Indicial Response	10
3.2 The Superposition Integral	11
3.3 Determination of $C_{m\dot{\alpha}}$ and $C_{m\dot{q}}$	12
3.4 Discussion	15
REFERENCES	17
FIGURES	19

FIGURE TITLES

Fig. 1.- Variation of $\frac{C_{I\alpha}}{\pi A/2}$ and \bar{x}_α with reduced aspect ratio, βA .

Fig. 2.- Variation of lift and moment coefficient correction terms with reduced aspect ratio, βA .

Fig. 3.- Comparison of theoretical and experimental damping coefficients for a triangular wing of aspect ratio 1.45.

Fig. 4.- Comparison of theoretical and experimental damping coefficients for a triangular wing of aspect ratio 2.

Fig. 5.- Comparison of theoretical and experimental damping coefficients for a triangular wing of aspect ratio 4.

Fig. 6.- Relationship between static stability and damping in pitch.

Fig. 7.- The indicial response.

Fig. 8.- Approximation of continuous angle-of-attack variation by means of step functions.

Fig. 9.- Motion which produces harmonic angle-of-attack variation.

Fig. 10.- Interpretation of the integrals appearing in the correlation constants.

Fig. 11.- Experimental correlation of effective static stability and damping in pitch.

SYMBOLS

A	aspect ratio
C_L	lift coefficient, $\frac{\text{lift}}{q_\infty S}$
C_m	pitching-moment coefficient, $\frac{\text{pitching moment}}{q_\infty S l}$
$F[]$	Fourier transform, $F[f(t)] = \int_0^\infty e^{i\omega t} f(t) dt$
M	Mach number, $\frac{V}{a_\infty}$
S	reference area (equals wing area in part 1)
V	flight speed
a_∞	speed of sound in free stream
c_0	wing root chord
i	$\sqrt{-1}$
l	reference length (equals c_0 in part 1)
$l_e(y)$	value of x at wing leading edge
m	slope of triangular wing leading edge, $m = \frac{A}{4}$
Δp	local loading (pressure on lower surface minus pressure on upper surface)
q	dimensionless pitching velocity, $\frac{\dot{\theta} l}{V}$
q_∞	dynamic pressure, $\frac{1}{2} \rho_\infty V^2$
t	time
u	dimensionless spanwise distance, $\frac{y}{mc_0}$
w	perturbation normal velocity at plane of wing
x,y,z	Cartesian coordinates fixed in wing with origin at wing leading edge; x positive rearward, z positive downward

\bar{x}_α	dimensionless location of center of pressure of lift due to angle of attack, $\frac{x_\alpha}{c_0}$
α	angle of attack
α_m	mean angle of attack
α_0	oscillation amplitude
β	$\sqrt{1-M^2}$
θ	angle of pitch
ρ_∞	mass density of free stream
ϕ	perturbation velocity potential
$\phi_x, \phi_{xx}, \text{etc.}$	$\frac{\partial \phi}{\partial x}, \frac{\partial^2 \phi}{\partial x^2}, \text{etc.}$
ϕ_c	correction potential
ψ	steady-state potential due to unit pitching velocity about y axis
χ	steady-state potential due to unit angle of attack
ω	circular frequency
$(\dot{\quad})$	$\frac{d(\quad)}{dt}$

When α , $\dot{\alpha}$, and q are used as subscripts with a lift or moment coefficient, a dimensionless derivative is indicated; thus

$$C_{m_\alpha} = \frac{\partial C_m}{\partial \alpha}, \quad C_{m_{\dot{\alpha}}} = \frac{\partial C_m}{\partial \frac{\dot{\alpha} l}{V}}, \quad C_{m_q} = \frac{\partial C_m}{\partial \frac{\theta \dot{l}}{V}}$$

ESTIMATION OF ROTARY STABILITY DERIVATIVES
AT SUBSONIC AND TRANSONIC SPEEDS

By Murray Tobak* and Henry C. Lessing*

National Aeronautics and Space Administration
Ames Research Center
Moffett Field, Calif.

1. INTRODUCTION

It is now generally recognized that modern aircraft, particularly tailless aircraft, can experience a significant loss of damping in the short-period pitching mode at transonic speeds. This loss has been traced to a reduction or even a change in sign of the damping-in-pitch parameter $C_{m_q} + C_{m_{\dot{\alpha}}}$. On the supersonic side of the transonic speed range a fairly complete understanding of the mechanism underlying the reduction of pitch damping has been made possible by the rapid development of theory in this range (cf. (1) and attendant bibliography). It is known, however, that the phenomena actually have their origins in the subsonic speed range; unfortunately, the great difficulty of the subsonic theoretical problem for finite-span wings has prevented a detailed study of these origins. Moreover, in the transonic speed range itself, and in fact, at all speeds, when flight conditions depart from those implicit in the range of applicability of a linearized theory, it is known that the aerodynamic forces and moments can become highly non-linear functions of angle of attack. Here again, the great difficulty of the theoretical problem has prevented our gaining an understanding of pitch-damping behavior under such circumstances. While it may not be

*Aeronautical Research Scientist

feasible to obtain explicit theoretical solutions in these cases, the possibility remains to formulate the problems so they relate closely to analogous problems in steady flow. The aerodynamics of steady flows being of fundamental importance in aircraft design, there exists a far greater fund of knowledge, both theoretical and experimental, relating to this field than exists for unsteady flows. Hence, if it is possible to relate an unsteady flow problem to an analogous problem in steady flow, one has the hope of bringing this fund of knowledge to bear.

This possibility will be examined for the two problems mentioned above; first, in the estimation by linear theory of pitch-damping coefficients of wings flying at subsonic speeds; second, in the estimation of pitch-damping coefficients when the aerodynamic forces and moments are non-linear functions of angle of attack.

2. ESTIMATION OF $C_{I\dot{\alpha}}$ AND $C_{m\dot{\alpha}}$ FOR WINGS AT SUBSONIC SPEEDS

Consider the first problem, the estimation of pitch damping of wings flying at subsonic speeds. As is well known, to a first order in frequency the pitch-damping coefficient is composed of two parameters; $C_{m\dot{q}}$, the pitching-moment coefficient proportional to constant pitching velocity, and $C_{m\ddot{\alpha}}$, the pitching-moment coefficient proportional to constant vertical acceleration. Now the analysis of $C_{m\dot{q}}$ already corresponds to that of a steady flow, namely the flow over a wing cambered and twisted to have a downwash distribution linearly dependent on chord-wise distance, x . Hence, all attention can be focused on the remaining parameter, $C_{m\ddot{\alpha}}$.

2.1 Solution to Potential Equation

To reduce the calculation for $C_{m\dot{\alpha}}$ to a steady flow problem, it is possible to adapt a simple device previously used extensively in calculating $C_{m\dot{\alpha}}$ at supersonic speed. The device was first introduced by Ribner and Malvestuto (2), who in turn credit it to C. S. Gardner. A solution is sought to the unsteady wave equation

$$\beta^2 \varphi_{xx} + \varphi_{yy} + \varphi_{zz} - \frac{2V}{a_\infty^2} \varphi_{xt} - \frac{1}{a_\infty^2} \varphi_{tt} = 0 \quad (1)$$

subject to the boundary conditions in the $z = 0$ plane

$$\left. \begin{aligned} w(x, y, 0) = \varphi_z(x, y, 0) = -\dot{\alpha} V t, \quad \text{on the wing} \\ \frac{\Delta p}{q_\infty} = \frac{4}{V} \left(\varphi_x + \frac{1}{V} \varphi_t \right)_{z=0} = 0, \quad \text{off the wing} \end{aligned} \right\} \quad (2)$$

Gardner has shown that a solution to Eq. (1) suitable for supersonic speed can be built of a combination of steady flow potentials; namely the potential due to steady unit pitching velocity ψ , and the potential due to steady unit angle of attack χ , in the combination shown in Eq. (3)

$$\begin{aligned} \varphi(x, y, z, t) = & -\frac{M^2}{\beta^2} \frac{\dot{\alpha} c_o}{V} \psi_{q=1}(x, y, z) + \dot{\alpha} \left(t + \frac{M^2 x}{V \beta^2} \right) \chi_{\alpha=1}(x, y, z) \\ & + \Phi_c(x, y, z) \end{aligned} \quad (3)$$

The adaptation of Eq. (3) to make it applicable to subsonic speeds consists only in adding a third steady flow potential, Φ_c . The necessity of this addition will be evident from inspection of the loading coefficient expression.

2.2 Loading Coefficient

The loading on the wing is obtained from Bernoulli's equation

$$\frac{\Delta p}{q_\infty} = \frac{4}{V} \left[\varphi_x(x, y, 0, 0) + \frac{1}{V} \varphi_t(x, y, 0, 0) \right] \quad (4)$$

and this leads to

$$\frac{\Delta p}{q_\infty} = \frac{\alpha c_o}{V} \left[-\frac{M^2}{\beta^2} \left(\frac{\Delta p}{q_\infty} \right)_{q=1} + \frac{M^2}{\beta^2} \frac{x}{c_o} \left(\frac{\Delta p}{q_\infty} \right)_{\alpha=1} + \frac{4}{\beta^2 V c_o} \chi_{\alpha=1} \right] + \left(\frac{\Delta p}{q_\infty} \right)_c \quad (5)$$

evaluated at $t = 0$. Now if the flight speed is supersonic and the wing has supersonic trailing edges, the wake is of no concern in calculating loading on the wing since it cannot affect conditions on the wing. In these circumstances, the first three terms in Eq. (5) constitute the solution for loading on the wing. For subsonic speeds, however, the Kutta condition must be invoked; this entails that loading be zero at the wing trailing edge, and of course, also in the wake. This condition is fulfilled by the first two terms in Eq. (5) but not by χ itself.

Writing χ as

$$\chi_{\alpha=1} = \frac{V}{4} \int_{l_e(y)}^x \frac{\Delta p}{q_\infty} (\xi, y)_{\alpha=1} d\xi \quad (6)$$

one sees that χ is a function of y in the wake, retaining at each station y the value it has at the wing trailing edge. This value is directly proportional to the span loading due to angle of attack, which may be presumed to be known. Hence, the potential Φ_c is added so that its loading contribution will cancel a spurious but known loading in the wake contributed by χ . In addition, since the boundary condition for downwash on the wing is already satisfied by ψ and χ alone, a second condition to be fulfilled by Φ_c is that $\partial\Phi_c/\partial z$ be zero at the wing surface. These two conditions suffice to determine the additional loading.

2.3 Solution for Triangular Wing

To avoid excessive mathematical development, it is merely stated here that after some manipulation, the problem for the correction loading can be reduced to finding the loading corresponding to a known downwash

dependent only on spanwise distance, y . Then by use of the reverse flow theorem, the lift and moment contributions are found relatively simply by spanwise integrations of this downwash distribution, multiplied by the reverse-flow span loadings due to angle of attack and pitching velocity. The form of the result as it applies to the triangular wing is given in Eq. (7).

$$\left. \begin{aligned} C_{L\dot{\alpha}} &= C_{Lq_0} + C_{m\dot{\alpha}_0} - \int_0^1 g(u) L(u)_{R,\alpha=1} du \\ C_{m\dot{\alpha}_0} &= C_{mq_0} + \int_0^1 \xi^2 d\xi \int_{-\xi}^{\xi} \frac{\Delta p}{q_\infty} (\xi, \eta)_{F,\alpha=1} d\eta + \int_0^1 g(u) L(u)_{R,q=1} du \end{aligned} \right\} (7)$$

where

$$g(u) = \frac{m^2}{\pi} \int_0^1 d\xi \int_{-\xi}^{\xi} \frac{\Delta p}{q_\infty} (\xi, \eta)_{F,\alpha=1} \frac{d\eta}{\sqrt{(1-\xi)^2 + \beta^2 m^2 (u-\eta)^2}}$$

$$L(u)_{R,\alpha=1} = \int_{|u|}^1 \frac{\Delta p}{q_\infty} (\xi, u)_{R,\alpha=1} d\xi$$

$$L(u)_{R,q=1} = \int_{|u|}^1 \frac{\Delta p}{q_\infty} (\xi, u)_{R,q=1} d\xi, \quad \text{axis at apex}$$

and the subscript 0 on the stability derivatives is meant to indicate that the terms are to be evaluated for an axis located at the wing apex. The subscripts F and R distinguish between loadings in forward and reverse flow, respectively.

2.4 Approximate Steady-State Loadings

In the form given, Eq. (7) is exact. It will be noted that the calculations involve the steady-state loadings due to angle of attack and pitching velocity, and the corresponding span loadings in reverse flow. Hence, the stated objective has been achieved. To complete the calculations, it would of course be most advisable to use experimental

data for these quantities, or secondly, exact theoretical solutions. Since probably, neither will be available in sufficient detail, approximations must be introduced at this stage. The calculation is a sensitive one, especially for pitching moment, in that it involves differences of numbers of approximately equal size. Therefore, in introducing approximate loadings it is advisable to use a set of loadings that is at least internally consistent, that is, a set that satisfies the reverse-flow theorem. In calculations for the triangular wing, it is possible to achieve this aim by a generalization of a technique introduced by Lomax and Sluder (3); namely, it is assumed that the loadings are those given by slender-wing theory, multiplied by a chordwise correction factor. The correction factor alters the slender-wing loadings both to account for compressibility and to comply with the Kutta condition. The loadings have the form given in Eq. (8).

$$\left. \begin{aligned} w_F = w_F(x) : \quad \frac{\Delta p}{q_\infty}(x,y)_F &= \frac{4}{V} f\left(\frac{x}{c_0}\right) \frac{\partial}{\partial x} \left[w_F(x) \sqrt{m^2 x^2 - y^2} \right] \\ w_R = w_R(x) : \quad \frac{\Delta p}{q_\infty}(x,y)_R &= - \frac{4}{V} \sqrt{m^2 x^2 - y^2} \frac{\partial}{\partial x} \left[w_R(x) f\left(\frac{x}{c_0}\right) \right] \end{aligned} \right\} \quad (8)$$

It will be noted that by virtue of the form of Eqs. (8), the integrand of the reverse-flow relation will form a perfect differential. The integration in x over the chord is then identically zero since f is zero at the trailing edge and the square root is zero at the leading edge. Hence satisfaction of the reverse-flow theorem is insured in a very simple way. The chordwise correction factor $f(x/c_0)$ may be obtained from results presented in (3).

Integrating the first of Eqs. (8) to obtain the steady-state stability derivatives in forward flow yields

$$\left. \begin{aligned} C_{L\alpha} &= \pi A \int_0^1 \xi f(\xi) d\xi \\ C_{m\alpha_0} &= -\pi A \int_0^1 \xi^2 f(\xi) d\xi \\ C_{Lq_0} &= \frac{3}{2} \pi A \int_0^1 \xi^2 f(\xi) d\xi \\ C_{mq_0} &= -\frac{3}{2} \pi A \int_0^1 \xi^3 f(\xi) d\xi \end{aligned} \right\} \quad (9)$$

Note that by virtue of Eqs. (8), C_{Lq_0} and $C_{m\alpha_0}$ are related simply by the factor $3/2$. It has also been found that the center of pressure of the lift due to pitching about the apex is given very closely by $9/8$ times the center of pressure of the lift due to angle of attack;* that is

$$\left. \begin{aligned} C_{Lq_0} &= -\frac{3}{2} C_{m\alpha_0} \\ \frac{C_{mq_0}}{C_{Lq_0}} &= \frac{9}{8} \frac{C_{m\alpha_0}}{C_{L\alpha}} \end{aligned} \right\} \quad (10)$$

Inserting Eqs. (8), (9) and (10) in Eqs. (7) leads to the following expressions for $C_{L\dot{\alpha}}$ and $C_{m\dot{\alpha}_0}$:

$$\left. \begin{aligned} C_{L\dot{\alpha}} &= \frac{1}{2} \bar{x}_\alpha C_{L\alpha} + C_L(g) \\ C_{m\dot{\alpha}_0} &= -\frac{9}{16} \bar{x}_\alpha^2 C_{L\alpha} + C_{m_0}(g) \end{aligned} \right\} \quad (11)$$

where

$$\begin{aligned} C_L(g) &= -\int_0^1 g(u) L(u)_{R, \alpha=1} du \\ C_{m_0}(g) &= \int_0^1 g(u) L(u)_{R, q=1, \text{apex}} du \end{aligned}$$

Curves of the parameters $C_{L\alpha}/(\pi A/2)$, \bar{x}_α , and the correction terms

*This result is also obtained using Lawrence's method (4) of computing the steady-state loadings.

$\beta^2 C_{L(g)} / (\pi A/2)$, $\beta^2 C_{m_0(g)} / (\pi A/2)$ are presented on Figs. 1 and 2.

From these results, all the stability derivatives can be obtained for triangular wings within the reduced aspect ratio range $0 < \beta A < 4$.

2.5 Empirical Corrections

Observe that by virtue of Eqs. (10) the expressions for the stability derivatives have been put almost completely in terms of $C_{L\alpha}$ and \bar{x}_α . It is to be expected that an improvement in accuracy and, for example, at least a partial account of wing-body interference effects could be realized by replacing $C_{L\alpha}$ and \bar{x}_α with values determined from experiments. The given results can be corrected in the following way. Let

$$\left. \begin{aligned} \mu &= \frac{C_{L\alpha \text{exp}}}{C_{L\alpha \text{th}}} \\ \nu &= \frac{\bar{x}_{\alpha \text{exp}}}{\bar{x}_{\alpha \text{th}}} \end{aligned} \right\} \quad (12)$$

Then

$$\left. \begin{aligned} C_{Lq_0} &= \frac{3}{2} \mu \nu \bar{x}_{\alpha \text{th}} C_{L\alpha \text{th}} \\ C_{mq_0} &= -\frac{27}{16} \mu \nu^2 \bar{x}_{\alpha \text{th}}^2 C_{L\alpha \text{th}} \\ C_{L\dot{\alpha}} &= \mu \left[\frac{1}{2} \nu \bar{x}_{\alpha \text{th}} C_{L\alpha \text{th}} + \mu C_{L(g)\text{th}} \right] \\ C_{m\dot{\alpha}_0} &= \mu \nu \left[-\frac{9}{16} \nu \bar{x}_{\alpha \text{th}}^2 C_{L\alpha \text{th}} + \mu C_{m_0(g)\text{th}} \right] \end{aligned} \right\} \quad (13)$$

These are the results which will be compared with results of experiments.

2.6 Comparison with Experiments

The theory as computed and corrected from Eqs. (13) is compared with experimental data for triangular wings of aspect ratio 1.45, 2, and 4 on Figs. 3 to 5. Experimental results for the $A = 1.45$ wing were obtained

at the Swedish Aeronautical Research Institute (5); those for the $A = 2$ and 4 wings, at the Ames Research Center (6), (7). On each figure, the damping coefficient as defined here is shown multiplied by a factor which converts it to comply with the defining units used in the experiment. It will be observed that in all three cases the accuracy of the theory is adequate. Note that the theory is capable of showing the reversal in trend of the damping coefficient that occurs at high subsonic Mach numbers; however, the reversal occurs sooner and more abruptly than predicted.

3. DAMPING IN PITCH IN THE PRESENCE OF NONLINEAR STEADY-STATE FORCES AND MOMENTS

The second problem mentioned previously will now be considered; namely, the estimation of pitch-damping coefficients when the aerodynamic forces and moments are nonlinear functions of angle of attack. The procedure will again be to formulate the problem to relate as closely as possible to conditions in steady flow. Evidence of the existence of such a relationship between steady and unsteady flow can be found in the literature; several experimental investigators (e.g., (8), (9)) have noted that when the static stability derivative $C_{m_{\alpha}}$ is a nonlinear function of angle of attack, the pitch-damping derivative $C_{m_q} + C_{m_{\dot{\alpha}}}$ is also nonlinear. More specifically, as indicated in Fig. 6, an increase (decrease) in static stability is accompanied by a decrease (increase) in pitch damping. Experimental results for several radically different configurations have confirmed the general nature of this relationship and the results, when cross plotted, in most cases have exhibited the linear correlation also shown in Fig. 6 and expressed as Eq. (14):

$$C_{m_q} + C_{m_{\dot{\alpha}}} = A + BC_{m_{\alpha}} \quad (14)$$

However, this information by itself is insufficient for the purpose of developing a rational estimation procedure, and the physical basis for such a relationship must be established.

3.1 The Indicial Response

In the analysis to follow, the physical basis for the relationship between pitch-damping and static stability will be illustrated through use of the concept of the indicial response. The indicial response of a system, by definition, is the response of the system to a disturbance in the form of a step function. As an illustration, Fig. 7 shows a step change in angle of attack $\Delta\alpha$. The indicial response which will be considered, also shown, is the resulting moment coefficient variation divided by the increment in angle of attack. It will be noted that the indicial response is not zero at time zero, but has a starting value which may be computed rather simply (e.g., (10)) from considerations of the initial momentum change imparted to the air immediately adjacent to the surface of the aerodynamic body. The response then proceeds to change with time, eventually reaching its steady-state value which has been indicated to be a function of angle of attack.

The following assumptions will be made concerning the indicial response: First, that the total response can be divided logically into two individual responses as indicated in the last sketch of Fig. 7. The first response is associated with the starting value, and falls to zero as the finite extent of the body alleviates the momentum initially imparted to the air. The second response is associated with the development of the flow pattern leading to the steady-state value. The starting value will be assumed independent of angle of attack. This assumption

is consistent with the results of linearized (10) and second-order aerodynamic theory for planar bodies (wings) and will be assumed to hold in general. Finally, the form of the response associated with the nonlinear steady-state value will be assumed to be independent of the nonlinearity. This assumption is based on the intuitive reasoning that the propagation of flow disturbances, that is, the mechanism by means of which the steady-state loading is attained, is independent of the form of the loading. The importance of the assumption lies in the fact that it retains the characteristic of the response of a linear system which permits the principle of superposition to be applied (11). With these assumptions the indicial response may be written as

$$\frac{\Delta C_m}{\Delta \alpha}(t, \alpha) = \frac{\Delta C_m}{\Delta \alpha}(0) f_1(t) + \frac{\Delta C_m}{\Delta \alpha}(\infty, \alpha) f_2(t) \quad (15)$$

where the limits of the functions f_1 and f_2 are zero and unity.

3.2 The Superposition Integral

In Fig. 8 an arbitrary angle-of-attack variation is shown, beginning with an initial value α_1 which has existed for an infinite period prior to time "zero." If the continuous variation is approximated by a series of step functions, then associated with each step is an indicial response such as previously discussed. The resulting moment variation is then given by the sum of the indicial responses,

$$\begin{aligned} C_m(t) &= C_m(0) + \frac{\Delta C_m}{\Delta \alpha}(t-t_1, \alpha_1)[\alpha_2 - \alpha_1] + \frac{\Delta C_m}{\Delta \alpha}(t-t_2, \alpha_2)[\alpha_3 - \alpha_2] + \dots \\ &= C_m(0) + \sum_n \frac{\Delta C_m}{\Delta \alpha}(t-t_n, \alpha_n) \Delta \alpha_n \end{aligned} \quad (16)$$

where each response is evaluated at the appropriate instant of time $(t-t_n)$ relative to its inception. Passing to the limit of an infinitesimal step

size then leads to Eq. (17):

$$C_m(t) = C_m(0) + \int_0^t C_{m\alpha}(t-\tau, \alpha(\tau)) \frac{d\alpha(\tau)}{d\tau} d\tau \quad (17)$$

Again one should note that the use of the superposition integral is possible only as a result of assuming an indicial response of unique form, containing the nonlinearity associated with α only as a multiplicative factor determining the magnitude of the response.

3.3 Determination of $C_{m\dot{\alpha}}$ and C_{mq}

As a result of the preceding development, it is possible to consider separately the two parameters C_{mq} and $C_{m\dot{\alpha}}$ which make up the total pitch damping. Attention will be focused here on $C_{m\dot{\alpha}}$, the pitching-moment coefficient proportional to vertical acceleration. The motion which leads to a moment proportional to $\dot{\alpha}$ but not to q is shown in Fig. 9 - harmonic plunging oscillations of an aerodynamic body at constant inclination to the mean flight path. The angle-of-attack variation is then given by

$$\alpha(t) = \alpha_m + \alpha_0 \sin \omega t \quad (18)$$

a harmonic variation of angle of attack of amplitude α_0 about a mean value α_m . If now the steady-state value of the indicial response is expanded in a Taylor series about the mean angle of attack α_m ,

$$C_{m\alpha}(\infty, \alpha) = C_{m\alpha}(\alpha_m) + \frac{dC_{m\alpha}}{d\alpha}(\alpha_m)[\alpha - \alpha_m] + \frac{1}{2} \frac{d^2 C_{m\alpha}}{d\alpha^2}(\alpha_m)[\alpha - \alpha_m]^2 + \dots \quad (19)$$

all the necessary equations have been developed for computing the total moment response to this motion. Substitution of Eqs. (15) and (19) in Eq. (17) and a little manipulation yields

$$\begin{aligned}
\Delta C_m(t) &= C_m(t) - C_m(0) = C_{m\alpha}(0) \int_0^t f_1(t-\tau) \frac{d\alpha(\tau)}{d\tau} d\tau \\
&+ a \int_0^t f_2(t-\tau) \frac{d\alpha(\tau)}{d\tau} d\tau + b \int_0^t f_2(t-\tau) \frac{d\alpha^2(\tau)}{d\tau} d\tau \\
&+ d \int_0^t f_2(t-\tau) \frac{d\alpha^3(\tau)}{d\tau} d\tau + \dots
\end{aligned} \tag{20}$$

where

$$a = C_{m\alpha}(\alpha_m) - \alpha_m \frac{dC_{m\alpha}}{d\alpha}(\alpha_m) + \frac{\alpha_m^2}{2} \frac{d^2C_{m\alpha}}{d\alpha^2}(\alpha_m) + \dots$$

$$b = \frac{1}{2} \frac{dC_{m\alpha}}{d\alpha}(\alpha_m) - \frac{\alpha_m}{2} \frac{d^2C_{m\alpha}}{d\alpha^2}(\alpha_m) + \dots$$

$$d = \frac{1}{6} \frac{d^2C_{m\alpha}}{d\alpha^2}(\alpha_m) + \dots$$

and $\Delta C_m(t)$ is the time-varying moment caused only by a time variation of angle of attack α . Any mean value of the moment has been subtracted as shown. If now the angle-of-attack variation given by Eq. (18) is introduced, $\Delta C_m(t)$ can be determined by a straightforward integration of Eq. (20). It is evident that because of the nonlinearity of the steady-state response, the response $\Delta C_m(t)$ to the harmonic angle of attack will not itself be harmonic, but will be instead a periodic function made up of components exhibiting some range of frequencies. However, only those components are of interest which are characterized by the frequency ω , since only those components are capable of doing work, or of being interpreted as an aerodynamic spring or aerodynamic mass. Application of the Fourier transform to $\Delta C_m(t)$ yields the desired components. A somewhat simpler and more direct approach is the application of the Laplace transform (11) to Eq. (20); reduction to the Fourier variable, ω , then yields the desired components directly. Either approach is straightforward and need not be detailed here. The final result is

$$\frac{F[\Delta C_m(t)]}{F[\alpha(t) - \alpha_m]} = C_{m\alpha_e} + i\omega[C_{m\alpha}(0)F_1(\omega) - C_{m\alpha_e}F_3(\omega)] \quad (21)$$

where

$$C_{m\alpha_e} = C_{m\alpha}(\alpha_m) + \frac{\alpha_0^2}{8} \frac{d^2 C_{m\alpha}}{d\alpha^2}(\alpha_m) + \dots \quad (22)$$

$$F_1(\omega) = \int_0^{\infty} f_1(t) e^{i\omega t} dt$$

$$F_3(\omega) = \int_0^{\infty} [1 - f_2(t)] e^{i\omega t} dt$$

The first term in Eq. (21) is a moment in phase with oscillatory angle of attack, and is therefore equivalent to an effective aerodynamic spring; hence the similarity in the notation to the usual designation of aerodynamic spring, $C_{m\alpha}$. The second term is complex through the Fourier transforms $F_1(\omega)$ and $F_3(\omega)$. The imaginary part is in phase with the rate of change of angle of attack, and is therefore proportional to $C_{m\dot{\alpha}}$. The real part is in phase with acceleration and can thus be identified as an aerodynamic mass. To the first order in frequency the aerodynamic mass contribution to the moment is zero. Also to the first order in frequency, $C_{m\ddot{\alpha}}$ can be expressed as

$$C_{m\ddot{\alpha}} = C + DC_{m\alpha_e} \quad (23)$$

where

$$C = \frac{V}{l} C_{m\alpha}(0) \int_0^{\infty} f_1(t) dt$$

$$D = -\frac{V}{l} \int_0^{\infty} [1 - f_2(t)] dt$$

The derivative $C_{m\ddot{\alpha}}$ is thus seen to have the linear correlation form originally given by Eq. (14), but the correlation relates to the effective value $C_{m\alpha_e}$ rather than the static value $C_{m\alpha}$. It will be seen later

that this form is the correct one. The constants C and D are functions of the starting value of the indicial response and integrals of the functions $f_1(t)$ and $f_2(t)$ which determine the form of the indicial response. The integrals are equal to the areas shown in Fig. 10.

The reader will note that the effective static stability $C_{m\alpha_e}$ given by Eq. (22) is the value which would be obtained by means of an experimental apparatus wherein the motion is inexorably forced and the aerodynamic moment component in phase with the angle of attack is measured. It can also be shown by the Kryloff-Bogoliuboff method (12) of nonlinear mechanics to be the value which would be obtained from frequency measurements of a tuned apparatus, that is, an apparatus which is forced to oscillate at its resonant frequency. It was by the latter method that the data to be presented subsequently were obtained.

A similar analysis for the derivative $C_{m\dot{q}}$ leads to the result

$$C_{m\dot{q}} = C_{m\dot{q}_e}(\alpha_m) \quad (24)$$

which states that, to first order in frequency, $C_{m\dot{q}}$ is equal to the effective steady-state value $C_{m\dot{q}_e}$ existing at the mean angle of attack α_m .

3.4 Discussion

From the previous development it is evident that the total pitch damping, as given by the sum of Eqs. (23) and (24),

$$C_{m\dot{q}} + C_{m\dot{\alpha}} = C_{m\dot{q}_e} + C + DC_{m\alpha_e} \quad (25)$$

should exhibit a linear correlation only if $C_{m\dot{q}_e}$ is independent of angle of attack, varies with angle of attack in the same manner as $C_{m\alpha_e}$, or is negligibly small. It is noted that those configurations investigated to date which have failed to exhibit a linear correlation have all been winged

configurations which would be expected to have a sizable value of C_{mq} relative to $C_{m\dot{\alpha}}$. Bodies of revolution, which would be expected to have a much smaller value of C_{mq} , have all correlated rather well. A typical example is shown in Fig. 11 where the pitch damping and the effective value of static stability are shown as functions of mean angle of attack for three oscillation amplitudes. These are data recently obtained at Ames Research Center for a body of revolution at a subsonic Mach number. The value of C_{mq} for this configuration is estimated to be quite small and, as can be seen, the data correlate very well. Note that, particularly in the region of greatest nonlinearity, the pitch damping varies with oscillation amplitude and would not, therefore, correlate with the single static stability curve given by $C_{m\dot{\alpha}}$. It is the simultaneous variation of the effective static stability $C_{m\alpha e}$ which leads to the correlation shown.

It appears, therefore, that a fairly sound understanding of the physical processes underlying a correlation between the dynamic stability derivative $C_{m\dot{\alpha}}$ and the static stability derivative $C_{m\alpha}$ has been attained. The constants in Eq. (23) indicate the quantities which must be determined in order to utilize these results in a rational estimation procedure - the starting value of the indicial response, and the characteristics of the response as determined by integrals of the functions $f_1(t)$ and $f_2(t)$. Work in this direction is now in progress.

REFERENCES

1. Miles, John W.: The Potential Theory of Unsteady Supersonic Flow. Cambridge University Press, England, 1959.
2. Ribner, Herbert S., and Malvestuto, Frank S., Jr.: Stability Derivatives of Triangular Wings at Supersonic Speeds. NACA Rep. 908, 1948.
3. Lomax, Harvard, and Sluder, Loma: Chordwise and Compressibility Corrections to Slender-Wing Theory. NACA Rep. 1105, 1952.
4. Lawrence, H. R.: The Lift Distribution on Low-Aspect-Ratio Wings at Subsonic Speeds. Jour. Aero. Sci., vol. 18, no. 10, Oct. 1951, pp. 683-695.
5. Orlik-Rückemann, Kazimierz, and Olsson, Carl O.: A Method for the Determination of the Damping-in-Pitch of Semi-Span Models in High-Speed Wind-Tunnels, and Some Results for a Triangular Wing. Aeronautical Research Inst. of Sweden (FFA), Rep. 62, 1956.
6. Emerson, Horace F., and Robinson, Robert C.: Experimental Wind-Tunnel Investigation of the Transonic Damping-in-Pitch Characteristics of Two Wing-Body Combinations. NASA MEMO 11-30-58A, 1958.
7. Beam, Benjamin H.: The Effects of Oscillation Amplitude and Frequency on the Experimental Damping in Pitch of a Triangular Wing Having an Aspect Ratio of 4. NACA RM A52G07, 1952.
8. Kemp, William B., Jr., and Becht, Robert E.: Damping-in-Pitch Characteristics at High Subsonic and Transonic Speeds of Four 35° Sweptback Wings. NACA RM L53G29a, 1953.

9. Lessing, Henry C., and Butler, James K.: Wind-Tunnel Investigation at Subsonic and Supersonic Speeds of the Static and Dynamic Stability Derivatives of an Airplane Model With an Unswept Wing and a High Horizontal Tail. NASA MEMO 6-5-59A, 1959.
10. Heaslet, Max. A., and Lomax, Harvard: Two-Dimensional Unsteady Lift Problems in Supersonic Flight. NACA Rep. 945, 1949.
11. Gardner, Murraray F., and Barnes, John L.: Transients in Linear Systems Studied by the Laplace Transformation. Volume 1, First Edition. New York, John Wiley and Sons, Inc., or London, Chapman and Hall, Limited, 1942, pp. 228 to 235.
12. Kryloff, N., and Bogoliuboff, N.: Introduction to Non-Linear Mechanics. A free translation by Solomon Lefschetz of excerpts from two Russian monographs. First Edition. Princeton, Princeton University Press, or London, Humphrey Milford, Oxford University Press, 1952, pp. 8 to 14.

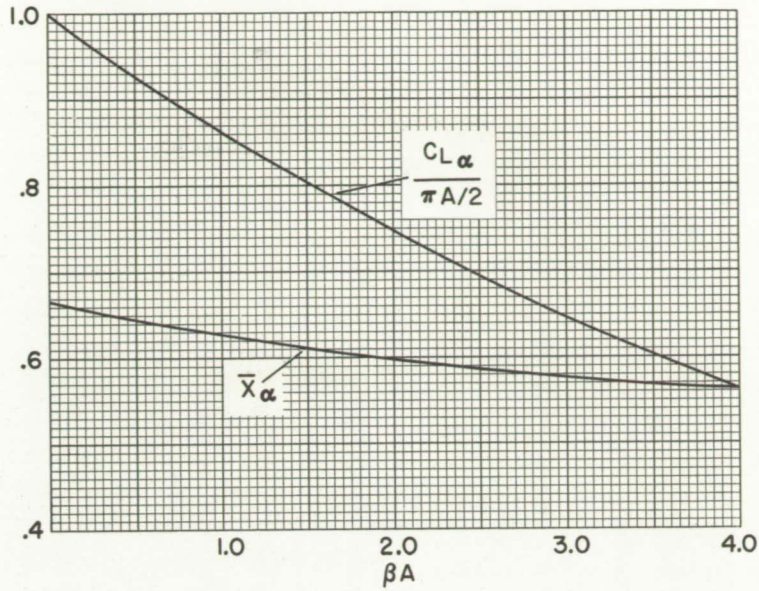


Fig. 1.- Variation of $\frac{C_{L\alpha}}{\pi A/2}$ and $\bar{\alpha}$ with reduced aspect ratio, βA .

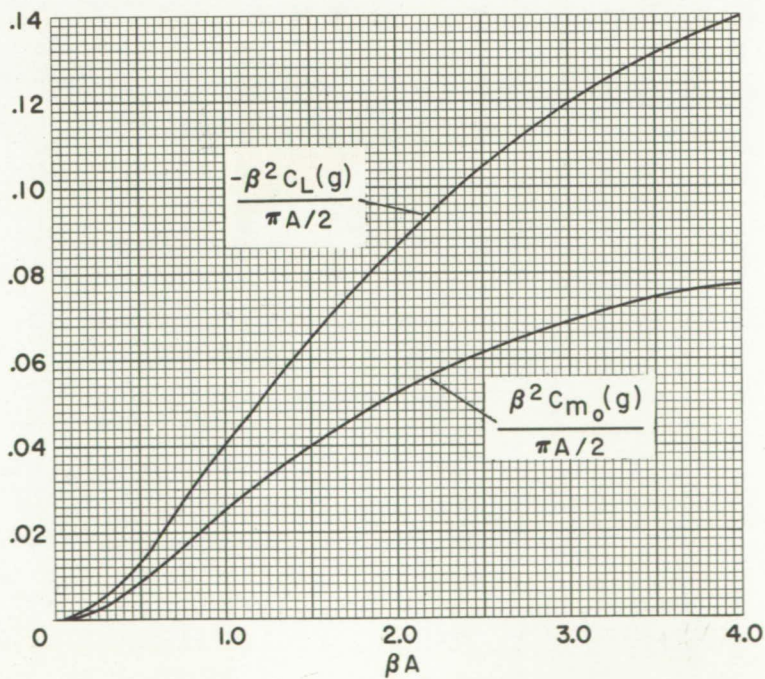


Fig. 2.- Variation of lift and moment coefficient correction terms with reduced aspect ratio, βA .

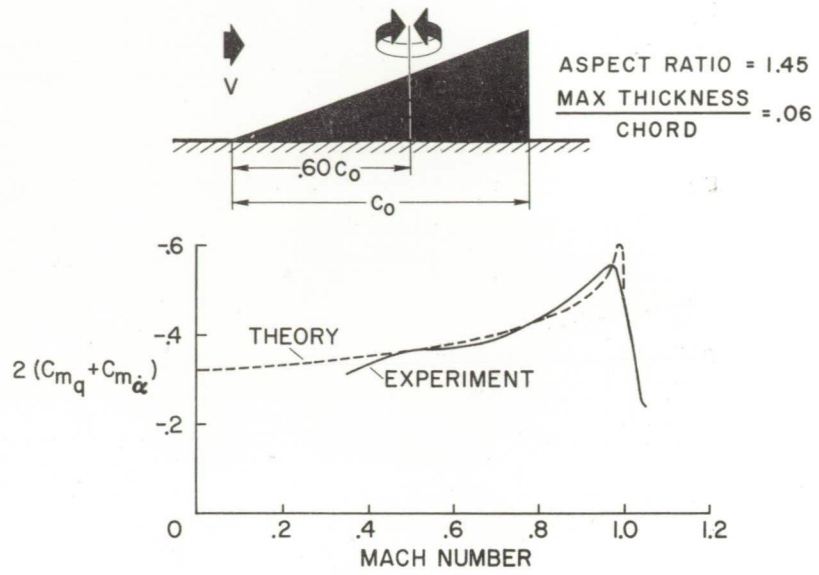


Fig. 3.- Comparison of theoretical and experimental damping coefficients for a triangular wing of aspect ratio 1.45.

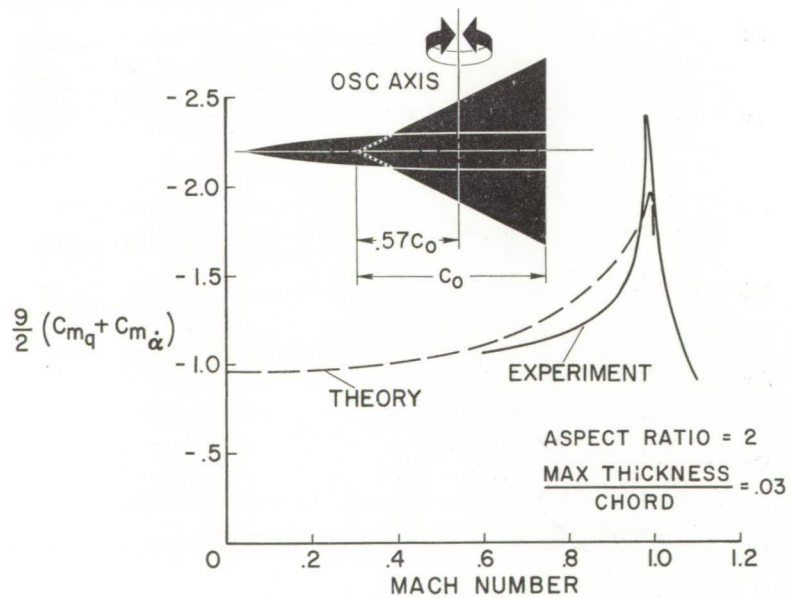


Fig. 4.- Comparison of theoretical and experimental damping coefficients for a triangular wing of aspect ratio 2.

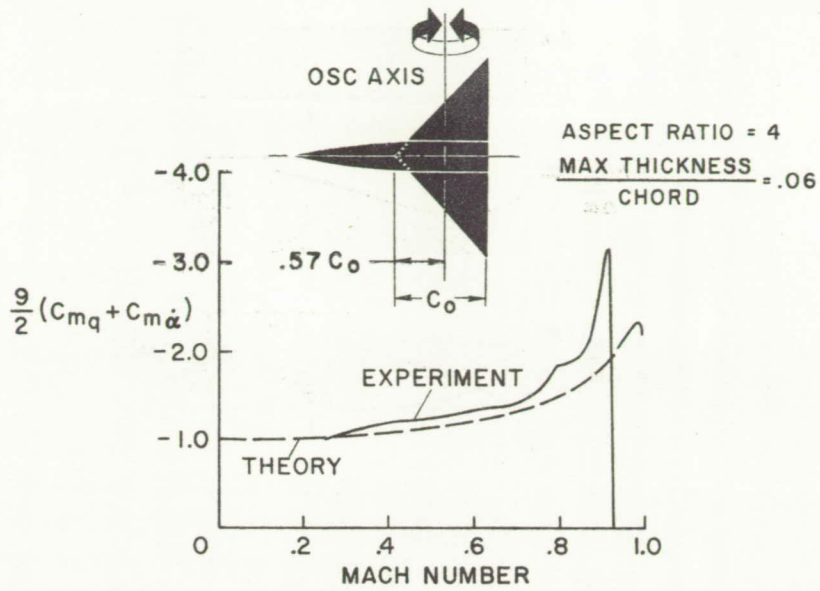


Fig. 5.- Comparison of theoretical and experimental damping coefficients for a triangular wing of aspect ratio 4.

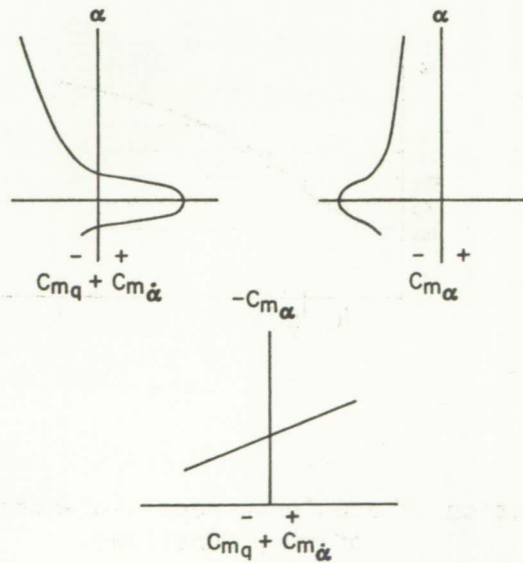


Fig. 6.- Relationship between static stability and damping in pitch.

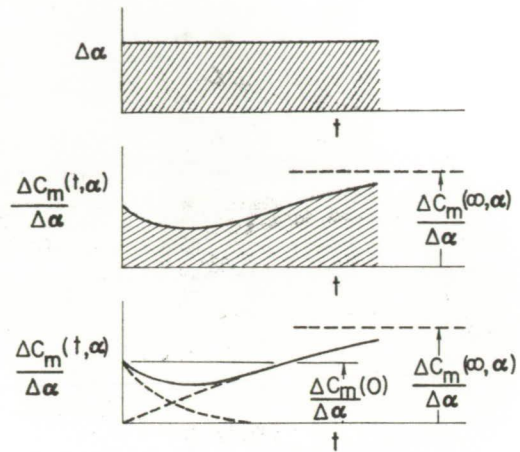


Fig. 7.- The indicial response

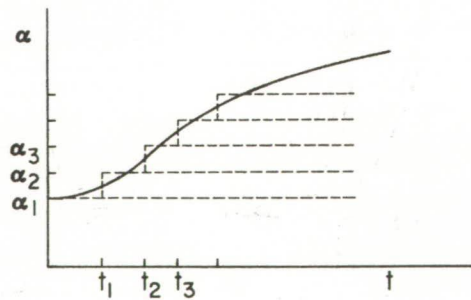


Fig. 8.- Approximation of continuous angle-of-attack variation by means of step functions.

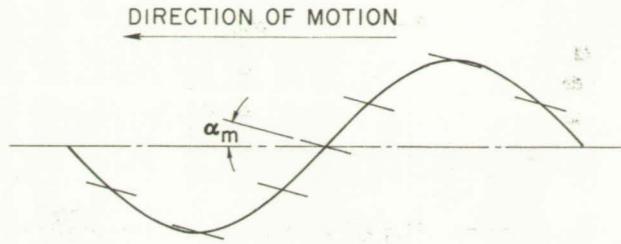


Fig. 9.- Motion which produces harmonic angle-of-attack variation.

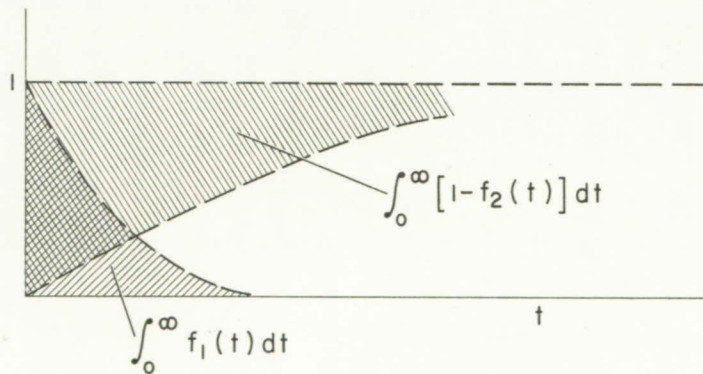


Fig. 10.- Interpretation of the integrals appearing in the correlation constants.

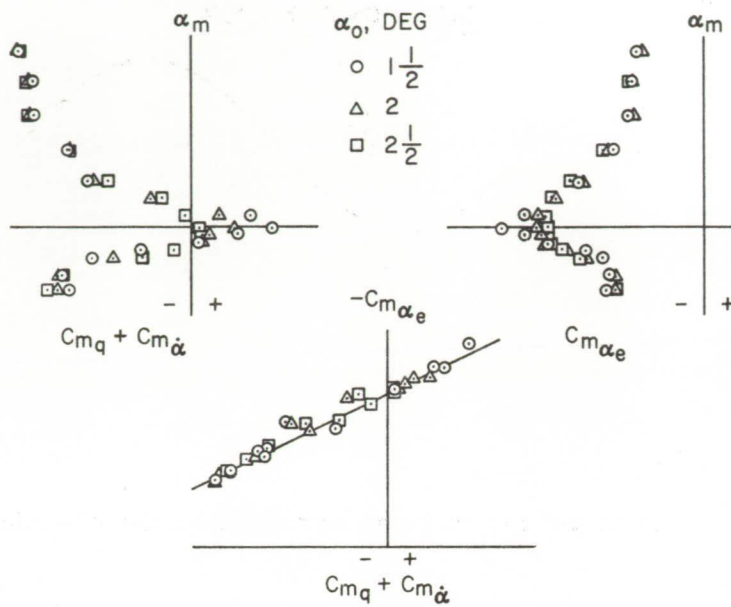


Fig. 11.- Experimental correlation of effective static stability and damping in pitch.